JOURNAL OF AIRCRAFT
Vol. 46, No. 4, July–August 2009

# Engineering Notes

*ENGINEERING NOTES are short manuscripts describing new developments or important results of a preliminary nature. These Notes should not exceed 2500 words (where a figure or table counts as 200 words). Following informal review by the Editors, they may be published within a few months of the date of receipt. Style requirements are the same as for regular contributions (see inside back cover).*

## Aerodynamic Characteristics of Forward and Aft Swept Arrow Wings

Lance W. Traub* and Jesse Lawrence†
*Embry Riddle Aeronautical University, Prescott, Arizona 86301-3720*

DOI: 10.2514/1.43098

### Introduction

DESPITE aerodynamic advantages, aeroelastic complications have precluded the wide-scale adoption of the forward swept wing planform [1]. Forward swept wings may demonstrate lift-dependent drag benefits due to spanwise load distributions that are closer to elliptic then an equivalent aft swept wing [2]. Fuselage-induced spanwise flow is also beneficial for forward swept wings; it reduces the effective sweep, whereas the opposite is true for aft swept wings [3]. The most apparent benefit of the forward sweep configuration is in lateral control; spanwise flow toward the root delays flow separation over the ailerons, whereas the opposite is true for aft swept wings [4].

Little information is available on the effect of highly swept wings with forward sweep where flow separation is enforced. Consequently, an investigation has been undertaken using a 65 deg sweep arrow wing with fore and aft extensions.

### Equipment and Procedure

Wind-tunnel tests were conducted in Embry Riddle's $2 \times 2$ ft blower wind tunnel. Force balance measurements were undertaken using a six-component NK sting balance. Balance output voltages were digitized using a National Instruments 16-bit A/D board. Each presented data point is the average of 5000 readings. Before testing, the balance's calibration was checked though the application of known weights.

The model's angle of attack was set within 0.1 deg using a feedback loop in conjunction with a Midori angle sensor. Wall corrections were applied using the method of Shindo [5], as well as that detailed in [6]. Testing was conducted at a freestream velocity of 25 m/s, yielding a Reynolds number of 180,000 based on the reference chord $c$ length of 0.127 m. During testing, the models were pitched to 28 deg in 2 deg increments.

The wind-tunnel models were manufactured from $\frac{1}{16}$-in. steel plate and were sheared to size. The plate edges were not beveled, however, the plate thickness would effectively enforce flow separation [7]. The wing planform had a leading- and trailing-edge sweep of 65 deg and was not tapered; the wing span of 0.254 m, in conjunction with a chord of 0.127 m, yielded an $AR$ of 2. The wing was attached to the sting mount either apex forward or aft to configure in the forward or aft sweep configuration. To evaluate the effect of strake-type attachments, as well as the interaction of the leading-edge vortices with a fuselage type extension, additional plates were manufactured. The plates were attached both ahead of (i.e., strake) as well as behind (aft extension) the wing in both the forward and aft swept configuration. The plate's sweep angle was 65 deg and extended to 38% of the span. The strakes/aft extension had an area 30% of the wings. The wing forms are displayed in the flow visualization section.

Presented coefficients are based upon a reference area corresponding to the wing's area, excluding the fore or aft extensions. Moments are taken about 50% of the total configuration chord.

### Results and Discussion

Figures 1–3 show a summary of the measured experimental data, as well as comparisons with theory. Theoretical computations were conducted using the vortex lattice code of Lamar [8]. The code has

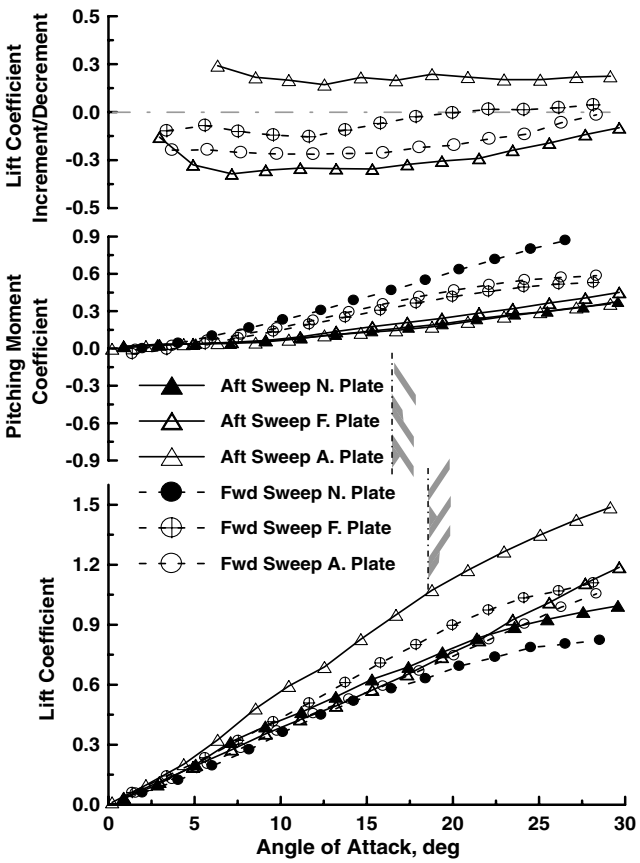


**Fig. 1 Effect of wing orientation and fore and aft extensions on measured lift, pitching moment, and surface loading.**

Received 6 January 2009; revision received 10 March 2009; accepted for publication 13 March 2009. 

*Associate Professor, Aerospace and Mechanical Engineering Department. Member AIAA.

†Undergraduate Student, Aerospace and Mechanical Engineering Department.

the capability to estimate vortex lift using the leading-edge suction analogy of Polhamus [9]. As may be seen in Fig. 1, the forward swept wing shows lower recorded lift than the aft swept wing for angles of attack greater than 4 deg. Attachment of the forward strake shows a greater lift increment for the forward swept wing then aft; the forward strake actually reduces lift in conjunction with aft sweep until high angles of attack (22 deg), above which it shows augmentation. Note that this result is representative for the particular strake geometry used in this investigation. Attachment of the aft extension shows a large lift increment for the aft swept wing, but only a marginal lift increase for the forward swept wing.

The pitching moment variation with angle of attack shows a positive moment slope for all wing configurations (see the middle inset of Fig. 1). This indicates that the wing's aerodynamic center is in front of the overall midchord for all configurations. The moment slope of the forward swept wings suggests low levels of loading over their aft sections and loading concentrated near the front of the wings. Such inferences will be clarified when observing the flow visualization results.

The upper inset of Fig. 1 shows the lift coefficient variation of the strake/aft plate composite configurations (based upon their actual or total areas) to the clean wings (i.e., no extensions), $(CL\text{composite} - CL\text{clean})/CL\text{clean}$. Consequently, the plot gives an indication of the efficiency of the area usage. As may be seen, all configurations excluding the aft swept wing with an aft extension show reduced average loading compared to the clean configurations (i.e., plot values are negative). Thus, for the present wing configurations, the addition of a strake or aft attachment generally shows a reduction in average loading. Notice that the decrement reduces with increasing incidence.

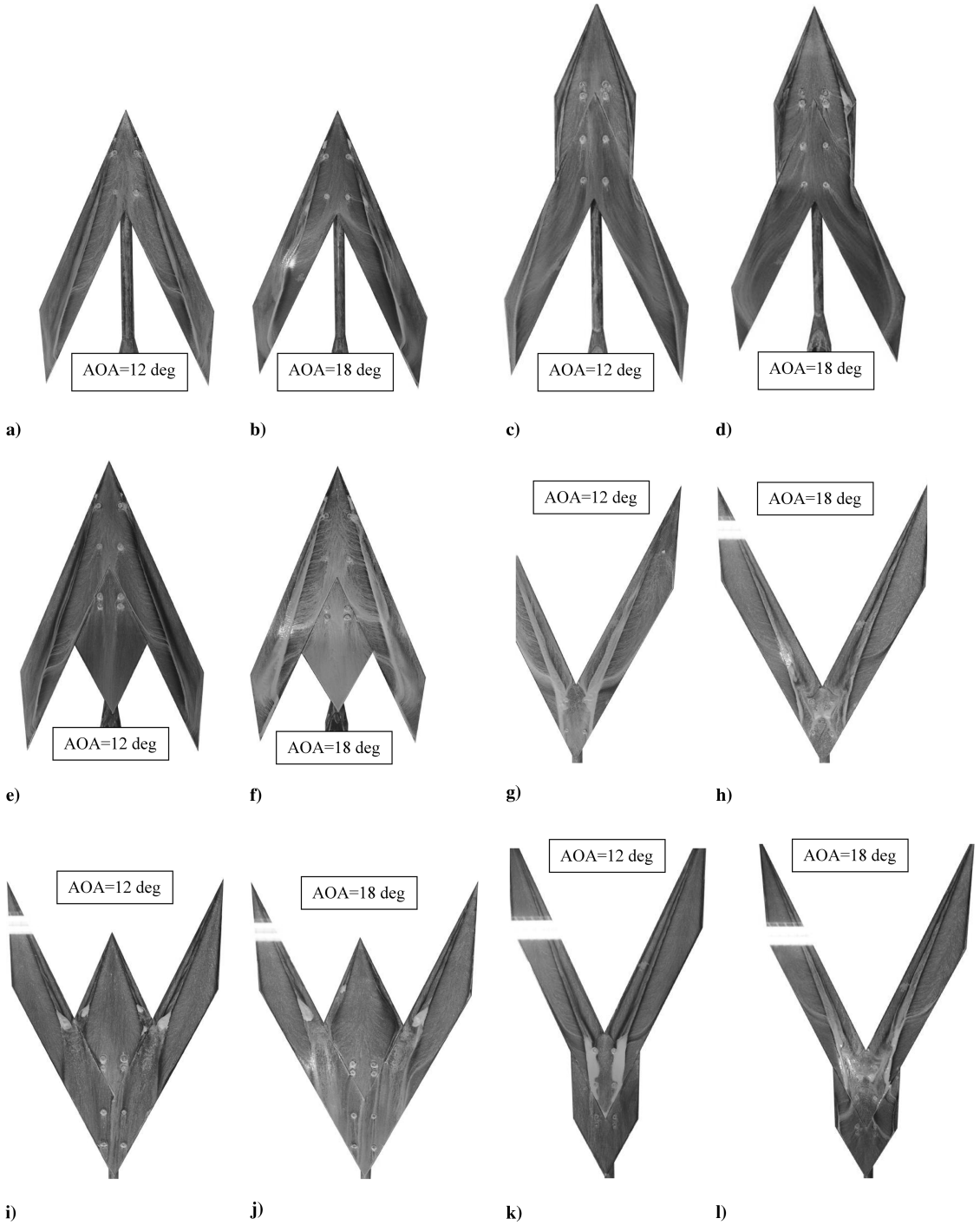


**Fig. 2 Surface skin-friction patterns over wing configurations. Freestream is from top to bottom.**

Figures 2a–2l show a summary of surface flow visualization (titanium dioxide suspended in kerosene and linseed oil) obtained at a wing incidence of 12 and 18 deg. The aft swept wing configurations show clear evidence of leading-edge and additional secondary and possible tertiary vortices. The secondary and tertiary vortices form due to boundary-layer separation caused by crossflow under the primary and secondary vortex suction peaks, respectively. The surface topology on the aft swept wing with and without the aft extension appears similar (Figs. 2a, 2b, 2e, and 2f). Without the plate, the flow is vortex dominated, with attachment of the free shear layer limited to inboard of the primary vortex near the wing apex. Attachment of the aft plate (Figs. 2e and 2f) provides area for shear layer attachment as well as attached axial flow. The skin-friction lines clarify the significant lift increment seen for this configuration in Fig. 1; the aft area allows for the benefit of the leading-edge vortex lift to be realized as the vortex shear layer is able to reattach. The aft swept wing at 18 deg incidence (Fig. 2b) shows an undulation in the secondary separation line that is not evident with aft plate attachment (Fig. 2f). Although this type of undulation is generally associated with boundary-layer transition [10], there does not appear to be a net outboard migration of this separation line. The undulation may be due to the upper surface boundary layer in this region originating from the trailing edge (as suggested by the skin-friction pattern), thus the boundary layer is thinner and better able to locally withstand an adverse pressure gradient (delayed separation) associated with passage underneath the primary vortex. Also note that, at 18 deg (Fig. 2b), the tertiary separation line is less well defined than at 12 deg, potentially due to bursting or off-surface displacement of the secondary separation vortices.

The aft swept wing with the strake (forward plate) shows skin-friction lines indicative of the presence of multiple strake vortices, as well as wing leading-edge vortices (primary, secondary, and tertiary). For the investigated angles, the wing and strake vortices do not appear to merge. The strake primary vortex appears to weaken over the aft portion of the wing, as suggested by the size and orientation of the sidewash skin-friction lines. This may be indicative of bursting or lift-off of the vortex from the surface. At 18 deg angle of attack, the aft portions of the wing show skin-friction patterns suggesting vortex breakdown (increased size of sidewash and reduced orientation to the freestream).

The forward swept wing shows the passage of leading-edge as well as secondary separation vortices (Figs. 2g and 2h). Also evident is a well-defined wing tip vortex. In comparison with the equivalent aft swept wings, the leading-edge vortices appear to be smaller, confined by other flow structures (wing tip and trailing-edge vortices) over the forward swept wings. The wing root section is seen to be essentially separated, indicative of the low recorded lift coefficients. Note that the root separation appears as a continuation of the secondary/tertiary separation lines. The geometric configuration also causes reducing proximity between the primary and secondary vortices and potential crowding and likely bursting of the secondary vortices. The topology also suggests that trailing-edge vorticity may roll up into the primary leading-edge vortices, reducing their circulation. Within the incidence range tested, the spanwise trajectory of the vortices appears invariant. The attachment of the strake (Figs. 2i and 2j) causes a displacement of the wing leading-edge vortices outboard (due to both sidewash from the strake vortex, as well as termination of the feeding sheet emanating from the leading edge). There does not appear to be a clear imprint of the strake vortices over the inboard wing section. Note that the wing secondary vortex separation lines terminate in a closed separation bubble, as do those over the strake. It is likely that the interference and increasing proximity between the vortices causes their bursting. It may also be that the velocities induced by the inclined leading-edge and strake primary vortices may serve to induce an upstream velocity component along the secondary strake and primary vortex core, respectively, causing a deceleration analogous to an adverse pressure gradient and potentially causing breakdown. Attachment of the aft plate (Figs. 2k and 2l) shows an extension of the separation described earlier for the clean forward swept wings (Figs. 2g and 2h) over the aft plate, explaining the poor performance of this configuration.

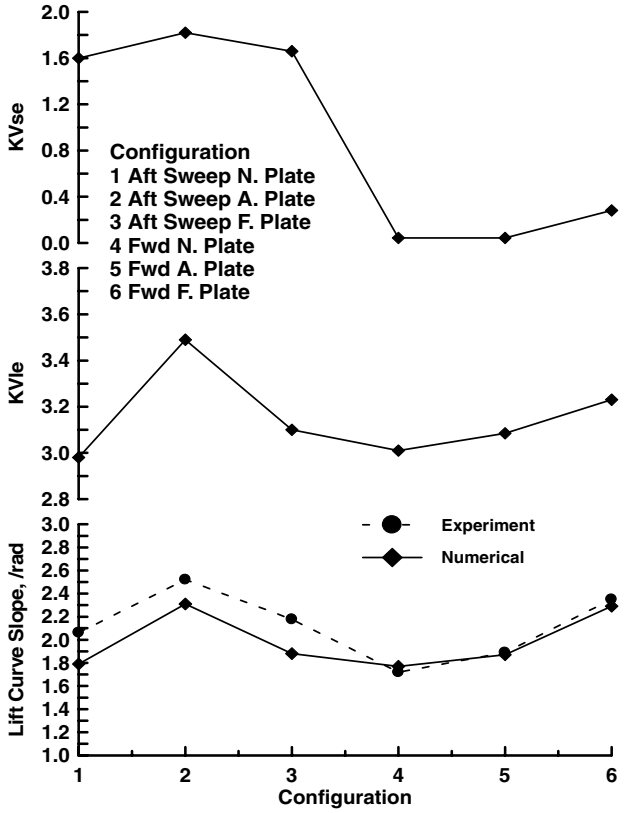


**Fig. 3 Effect of configuration on numerically determined lift parameters.**

Figure 3 shows a summary of salient numerically estimated attached flow and vortex lift parameters (KVle and KVse, KV relates to the rate of change of the leading-edge or side-edge suction with the square of the angle of attack). The data show close accord between the experimental and theoretical lift curve slopes, with the forward swept wing variants showing the best agreement. Notice that the numerical lift curve slopes show equivalent values for a configuration run forward or backward, that is, 1 and 4, 2 and 6, and 3 and 5. This

**Table 1 Experimental and numerical data summary**

| Config. | $CL\alpha$, exp, /rad | $CL\alpha$, theory, /rad | $e_{\text{exp}}$ | $e_{\text{exp}} = CL\alpha/\pi AR$ | $e_{\text{theory}}$ | $Cm\alpha$, exp | $Cm\alpha$, theory |
|---|---|---|---|---|---|---|---|
| AS-NP | 2.06 | 1.79 | 0.34 | 0.33 | 0.43 | −1.5 | −1.56 |
| AS-AP | 2.52 | 2.31 | 0.53 | 0.4 | 0.53 | −1.53 | −1.55 |
| AS-FP | 2.19 | 1.88 | 0.3 | 0.35 | 0.45 | −1.0 | −2.2 |
| FS-NP | 1.72 | 1.77 | 0.31 | 0.27 | 0.38 | 0.85 | 0.66 |
| FS-AP | 1.90 | 1.87 | 0.3 | 0.3 | 0.39 | 0.8 | 0.63 |
| FS-FP | 2.35 | 2.29 | 0.36 | 0.37 | 0.46 | 1.16 | 1.0 |

[a]$AS$ = aft sweep, $FS$ = forward sweep, $NP$ = no plate, $AP$ = aft plate, $FP$ = front plate, $CL\alpha$ = lift curve slope, $Cm\alpha$ = moment curve slope

result follows from Heaslet and Spreiter's [11] reciprocal relations. It does not, however, apply to drag, as the leading-edge suction may vary depending on which way the wing is flown. The leading-edge vortex lift parameter KVle is somewhat similar for all configurations except the aft swept wing with the aft plate, which shows an increase. Note that this parameter does not show fore and aft symmetry for a given configuration. The side-edge suction parameter KVse suggests that the forward swept wings develop negligible vortex lift along their side edges, as mentioned earlier.

Table 1 shows a data summary of significant aerodynamic parameters. Agreement between theory and experiment is generally good. The Oswald efficiency factor $e$ was calculated by linearizing the drag polar and fitting a linear regression to the resulting plot. For a flat plate with zero leading-edge suction, $e$ is given by $CL\alpha/\pi AR$. Consequently, if the lift curve slope varies, so does $e$. As shown in Table 1, $e$ calculated using this formula shows close accord with $e$ calculated from the drag polar, as may be expected noting the approximately linear behavior of the lift curve slopes in Fig. 1. The only marked exception is the aft swept wing with aft plate. The significant vortex lift developed by this configuration results in a higher efficiency than based on the attached flow lift curve slope.

## Conclusions

An experimental investigation has been conducted to characterize the behavior of a thin 65 deg sweep $AR = 2$ untapered arrow wing. The wing was tested in both forward and aft sweep configurations. The effect of fore and aft root extensions were also evaluated. Both the forward and aft swept wing configurations showed vortex dominated flows, with the forward swept configurations showing significant loss of lift compared to the aft swept wings. Surface flow visualization showed large extents of flow separation near the wing root of the forward swept wings as well as smaller leading-edge vortices compared to the aft swept wings. The forward extension (a strake) was beneficial when used in conjunction with the forward swept wing but detrimental when used with the aft swept wing. The opposite results were seen for the aft extension.

## Acknowledgments

The authors would like to thank Kali Schroeder, Niels Morck, Alex Morgan, and Adam Rodriguez for undertaking the wind-tunnel tests.

## References

[1] Uhuad, G. C., Weeks, T. M., and Large, R., "Wind Tunnel Investigation of the Transonic Aerodynamic Characteristics of Forward Swept Wings," *Journal of Aircraft*, Vol. 20, No. 3, 1983, pp. 195–202. doi:10.2514/3.44853

[2] Breitsamter, C., and Laschka, B., "Vortical Flowfield Structure at Forward Swept-Wing Configurations," *Journal of Aircraft*, Vol. 38, No. 2, 2001, pp. 193–207. doi:10.2514/2.2758

[3] Redeker, G., and Wichmann, G., "Forward Sweep: A Favorable Concept for a Laminar Flow Wing," *Journal of Aircraft*, Vol. 28, No. 2, 1991, pp. 97–103. doi:10.2514/3.45997

[4] Arnott, A. D., and Bernstein, L., "The Aerodynamic Interaction at the Junction Between a Forward-Swept Wing and a Plate," *The Aeronautical Journal*, Vol. 104, No. 1032, Feb. 2000, pp. 67–88.

[5] Shindo, S., "Simplified Tunnel Correction Method," *Journal of Aircraft*, Vol. 32, No. 1, 1995, pp. 210–213. doi:10.2514/3.46705

[6] Barlow, J. B., Rae, W., and Pope, A., *Low-Speed Wind Tunnel Testing*, 3rd ed., Wiley-Interscience, New York, 1999, pp. 367–425.

[7] Kegelman, J. T., and Roos, F. W., "Effects of Leading-Edge Shape and Vortex Bursts on the Flowfield on a 70-Deg-Sweep Delta Wings," AIAA Paper 89-0086, Jan. 1989.

[8] Lamar, J. E., "Extension of the Leading-Edge Suction Analogy to Wings with Separated Flow Around the Side Edges at Subsonic Speeds," NASA TR R-428, 1974.

[9] Polhamus, E. C., "Prediction of Vortex-Lift Characteristics by a Leading Edge Suction Analogy," *Journal of Aircraft*, Vol. 8, No. 4, 1971, pp. 193–199. doi:10.2514/3.44254

[10] Traub, L. W., "Effects of Spanwise Camber on Delta Wing Aerodynamics: An Experimental and Theoretical Investigation," Ph.D. Dissertation, Aerospace Engineering Dept., Texas A&M Univ., College Station, TX, May 1999.

[11] Heaslet, M. A., and Spreiter, J. R., "Reciprocity Relations in Aerodynamics," NACA Rept. 1119, 1953, p. 16.